Asian Journal of Physical and Chemical Sciences

7(1): 1-14, 2019; Article no.AJOPACS.46301
ISSN: 2456-7779

Heat Transfer of Mixed Convection Electroconductivity Flow of Copper Nanofluid with Different Shapes in a Porous Micro Channel Provoked by Radiation and First Order Chemical Reaction

Alalibo T. Ngiangia[1*] and Nelson N. Akaezue[1]

[1]Department of Physics, University of Port Harcourt, P.M.B. 5323, Choba, Port Harcourt, Nigeria.

Authors' contributions

This work was carried out in collaboration between both authors. Both authors read and approved the final manuscript.

Article Information

DOI: 10.9734/AJOPACS/2019/46301
Editor(s):
(1) Dr. Mustafa Boyukata, Professor, Department of Physics, Bozok University, Turkey.
Reviewers:
(1) Bunonyo, Wilcox Kubugha, Federal University Otuoke, Nigeria.
(2) Sher Muhammad, Islamia College Peshawar, Pakistan.
Complete Peer review History: http://www.sdiarticle3.com/review-history/46301

Original Research Article

Received 16 October 2018
Accepted 02 January 2019
Published 19 January 2019

ABSTRACT

This paper investigates the theoretical description of different shapes of copper nanoparticle in water based fluid. Analytical solution of the governing hydrodynamic equations and graphs plotted. The work showed that heat transfer is rapid due to the presence of radiation. Increase in radiation and chemical reaction also led to a corresponding increase in the temperature and concentration profiles of the nanofluid respectively. For the velocity profile of the nanofluid, only the nanoparticles volume fraction increases the velocity profile of the copper nanofluid. Reynolds number, Grashof's number and electroconductivity, result to decrease in the velocity profile of the same. The effect of Nusselt number, Sherwood number and skin friction on the nanofluid are also determined.

Keywords: Heat transfer; copper; nanofluid; porous channel; water based fluid.

**Corresponding author: E-mail: alalibo.ngiangia@uniport.edu.ng, analemnkem@gmail.com;*

NOTATION

ρ_{nf} : density of nanofluid
P : pressure of fluid
U : dimensionless fluid velocity
μ_{nf} : dynamic viscosity of nanofluid
$(\rho\beta)_{nf}$: thermal expansion coefficient of nanofluids due to temperature
σ_{∞} : constant fluid electronconductivity
U : plate velocity
k_0 : porosity of the medium
k_{nf} : thermal conductivity of nanofluid
Q : radiative heat f lux
g : acceleration due to gravity
k_f : thermal conductivity of base fluid
ϕ : nanoparticles volume fraction
ρ_f : density of base fluid
ρ_s : density of nanoparticles
$(\rho C_p)_{nf}$: heat capacitance of nanofluids
β_s : volumetric coefficient of nanoparticles
β_f : volumetric coefficient of base fluid
$(C_p)_f$: specific heat capacity of base fluid
$(C_p)_s$: specific heat capacity of nanoparticles
C' : concentration of fluid
C : dimensionless concentration of fluid
T : temperature of fluid
θ : dimensionless temperature of fluid
Re : Reynolds number
Pe : Peclet number
Gr_T : thermal Grashof number
Gr_C : concentration Grashof number
N : dimensionless radiation term
k_{∞} : dimensionless chemical reaction term
k_r^2 : chemical reaction term
λ_n : thermal conductivity ratio
D_{nf} : molecular diffusivity
u' : fluid velocity

1. INTRODUCTION

Thermal conductivity of heat transfer in fluids is important in the development of energy efficient heat transfer equipment. Conventional heat transfer fluids such as water, oil, ethylene glycol mixtures to mention few, are poor heat transfer fluids. With global need for improvement, to develop advanced heat transfer fluids with significantly higher thermal conductivities than those presently available is of utmost necessity. Touloukian et al. [1] has opined that at room temperature, metals in solid form have orders of magnitude higher than those of solids. The new class of heat transfer fluids that are engineered by suspending nanometer-sized particles in conventional heat transfer fluids whose averaged sized particles is below 50nm is termed nanofluids Choi [2] The reality is that in today's science and technology, size does matter, therefore modern fabrication technology provides great opportunity to actively process materials at the micro and nanometer scales. The impact of this new heat transfer technology is important due to its performance in thermal conductivity and viscosity which led to improved heat transfer and stability, reduced pumping power, minimal clogging and miniaturized systems as well as cost and energy savings (Choi et al. [3] and [4]). The different composition of nanoparticles in base fluids to form nanofluids has its application in power generation and electronic equipment just to mention few. The applications of nanofluids is predicated on the desirable propreties or qualities following Mukherjee and Paria [5] as follows (i) rapid increase in thermal conductivity (ii) ultrafast heat transfer ability (iii) reduce pumping power (iv) reduce friction coefficient (v) reduce clogging in microchanels (vi) improved stability than other colloids and (vii) improved lubrication. Feng et al. [6], examined the preparation of gold, silver and platinum nanofluids using aqueous organic phase transfer method. Yu et al. [7], Wei and Wang [8] and Zhu et al. [9], prepared Copper oxide nanofluid and use amoniun citrate to prevent the growth and aggregation of nanoparticles, resulting in a stable CuO aqueous nanofluid with higher thermal conductivity. Other works such as Hwang, et al. [10] and Li et al. [11], used spectral analysis method to detect stability of nanofluids. Experimental and theoretical studies are abounded on conductivity, viscosity and stability of nanofluids and its aggregate nanoparticles. Recently, Hussain et al. [12], Muhammad et al. [13], Muhamed et al. [14] and Muhammad et al. [15], examined nanofluid materials and made far reaching deductions from their findings. The model proposed by Hamilton and Crosser [16] to predict the thermal conductivity of nanofluid, containing large agglomerated particles and that

obtained from experimental results were compared and it fits well, but divergence is observed at low volume fractions. The implication of this observation is that particle size and shape dominate thermal conductivity of nanofluids (Li [17]). Studies on nanoparticles of spherical shapes are many but limited in applications and significance, Aaiza et al. [18]. As a result of this assertion, a non spherical shaped nanoparticle is chosen for this study in four different shapes, namely, platelet, cylinder, blade and brick. The choice of non spherical shape nanoparticle is predicated on the work of Aaiza et al. [18], where they mentioned desirable properties in cancer treatment. Asma et al. [19], studied free convection flow of nanoparticles including ramped wall temperature using five different types of spherical shape nanoparticles and reported that the solution of the governing equations was exact. Heat transfer due to mixed convection is experienced in many physical situations and occur as the flow in a channel due to the process of heating or cooling of the channel walls. This experience is a combination of free convection and forced convection. Some researches have been reported, they include Sebdani et al. [20], Sheikhzabeh et al. [21], Nadeem and Saleem [22] and Al-Salem et al. [23] in which mixed convection and nanofluid were discussed in different nanoparticles shape and configurations. Aaiza et al. [18], investigated water based nanofluid and ethylene glycol based nanofluid and reported that viscosity and thermal conductivity are the most prominent parameters responsible for different results of velocity and temperature. The present study is to examine the effect of first order chemical reaction and electroconductivity on radiative heat transfer in mixed convection flow in a micro porous channel with different shapes of copper (Cu) in water based nanofluid. The Cu in water based nanofluid preparation and sphericity is reported in Yimin and Li [24]. The reason is that Cu as a nanoparticle, possesses higher thermal conductivity and stability than other nanofluids. The focus is to consider non spherical shaped nanofluid under the no slip boundary conditions with bounding walls of the channel at rest, the upper wall in motion and lower at rest and both walls are in motion. Solutions to velocity, temperature and concentration profile with graphical results and parameters of interest discussed, which is an extension of the work of Aaiza et al. [18]

2. FORMULATION OF THE PROBLEM

The assumption of the effect of induced magnetic field is small. Therefore, it is neglected. Also the usual Boussinesq approximation is assumed. The no slip condition at the boundary wall is considered. The x-axis is taken along the flow and y-axis is taken normal to the flow direction. The governing hydrodynamic equations are given as:

$$\rho_{nf}\frac{\partial u'}{\partial t'} = -\frac{\partial p}{\partial x'} + \mu_{nf}\frac{\partial^2 u'}{\partial y^2} - u\left(\frac{\sigma_\infty}{U} + \frac{\mu_{nf}}{k_0}\right) + \left(\rho\beta_T\right)_{nf} g\left(T - T_0\right) + \left(\rho\beta_c\right)_{nf} g\left(C - C_0\right) \tag{1}$$

$$\left(\rho C_p\right)_{nf}\frac{\partial T}{\partial t'} = k_{nf}\frac{\partial^2 T}{\partial y^2} - \frac{\partial q}{\partial y} \tag{2}$$

$$\left(\rho C_p\right)_{nf}\frac{\partial C'}{\partial t'} = D_{nf}\frac{\partial^2 C'}{\partial y^2} - k_r^2 C' \tag{3}$$

With the boundary conditions

$$u'(0,t) = 0, \quad u'(d,t) = 0, \tag{4}$$

$$T(0,t) = T_0 \ , \qquad T(d,t) = T_w \tag{5}$$

$$C'(0,t) = C_0 \ , \qquad C'(d,t) = C_w \tag{6}$$

Following Boricic et al. [25], the fluid electroconductivity is assumed to be of the form $\sigma_\infty\left(1-\frac{u'}{U}\right)$ but for physical exigency and mathematical amenability, it is approximated to the form in equation (1) Ngiangia and Harry [26].

According to a model proposed by Hamilton and Crosser [16], the thermal conductivity and dynamic viscosity is assumed valid for both spherical and non spherical shapes nanoparticles. The model is stated as

$$\mu_{nf} = \mu_f\left(1 + a\phi + b\phi^2\right) \tag{7}$$

$$\frac{k_{nf}}{k_f} = \frac{k_s + (n-1)k_f + (n-1)(k_s - k_f)\phi}{k_s + (n-1)k_f - (k_s - k_f)\phi} \tag{8}$$

where $n = \frac{3}{\psi}$ is the empirical shape factor and ψ is the sphericity, a ratio of surface area of sphere to surface area of real particle with equal volumes as in Table 1 with a and b as constant empirical shape factors.

Another expression by Wasp [27] to determine the effective thermal conductivity of solid-liquid mixture is given as

$$\frac{k_{eff}}{k_f} = \frac{k_s + 2k_f - 2\phi(k_f - k_s)}{k_s + 2k_f - \phi(k_f - k_s)} \tag{9}$$

This is a special case of equation (8) with sphericity 1.0

From equations (1), (2) and (3), ρ_{nf}, $(\rho\beta)_{nf}$ and $(\rho C_p)_{nf}$ following Asma et al. [19] is derived as

$$\begin{aligned} \rho_{nf} &= (1-\phi)_{\rho_f} + \phi\rho_s \\ (\rho\beta)_{nf} &= (1-\phi)(\rho\beta)_f + \phi(\rho\beta)_s \\ (\rho C_p)_{nf} &= (1-\phi)(\rho C_p)_f + \phi(\rho C_p)_s \end{aligned} \tag{10}$$

In the work of Makinde and Mhone [28], the plates temperature T_0 and T_w are usually high and produces radiative heat transfer. According to Cogley et al. [29], for optically thin medium with relatively low density, the radiative heat flux is given by

$$\frac{\partial q}{\partial y} = 4\delta^2(T - T_0) \tag{11}$$

where δ is the radiation absorption coefficient

Substituting equation (11) into equation (2) and using the following dimensionless Variables

$$x = \frac{x'}{d}, y = \frac{y'}{d}, u = \frac{u'}{U}, t = \frac{t'U}{d}, \frac{\partial p}{\partial x'} = \lambda\exp(i\omega t), \theta = \frac{T - T_0}{T_w - T_0}, \mathrm{Re} = \frac{Ud}{\mu_f}$$

$$k = \frac{k_0}{d^2}, Gr_T = \frac{g\beta_f d^2(T_w - T_0)}{\mu_f U}, Gc_T = \frac{g\beta_c d^2(C' - C_0)}{\mu_f U}, \sigma_0 = \frac{\sigma_\infty \mu_f dt}{U}$$

$$N = \frac{4\delta^2 d^2}{k_f}, Pe_T = \frac{Ud(\rho C_p)_f}{k_f}, Pe_C = \frac{Ud(\rho C_p)_f}{D_{nf}}, k_\infty = \frac{k_r^2 T_0}{\sigma_\infty U^2}, \lambda_n = \frac{k_{nf}}{k_f}$$

Further, we define

$$w_1 = (1-\phi) + \phi\frac{\rho_s}{\rho_f} \quad w_2 = \left(1 + a\phi + b\phi^2\right) \quad w_3 = (1-\phi)\rho_f + \phi\frac{(\rho\beta)_s}{\beta_f}$$

$$w_4 = \left[(1-\phi) + \phi\frac{(\rho C_p)_s}{(\rho C_p)_f}\right] \quad a_1 = w_1\,\mathrm{Re} \quad a_2 = \sigma_0 + \frac{w_2}{k} \quad a_3 = w_3 Gr_T$$

$$a_4 = w_3 Gr_c, c_1 = \frac{Pe_c w_4}{\lambda_n} \quad b_1 = \frac{Pe_T w_4}{\lambda_n} \quad b_2 = \frac{N}{\lambda_n}, c_2 = \frac{k_\infty}{\lambda_n},$$

then equations (1), (2) and (3) takes the form

$$a_1 \frac{\partial u}{\partial t} = \lambda\varepsilon \exp(i\omega t) + w_2 \frac{\partial^2 u}{\partial y^2} - a_2 u + a_3\theta + a_4 C \tag{12}$$

$$b_1 \frac{\partial \theta}{\partial t} = \frac{\partial^2 \theta}{\partial y^2} - b_2\theta \tag{13}$$

$$c_1 \frac{\partial C}{\partial t} = \frac{\partial^2 C}{\partial y^2} - c_2 C \tag{14}$$

Subject to the boundary conditions

$$u(0,t) = 0, \quad u(1,t) = 1 \qquad t > 0 \tag{15}$$

$$\theta(0,t) = 0, \qquad \theta(1,t) = 1 \qquad t > 0 \tag{16}$$

$$C(0,t) = 0, \quad C(1,t) = 1 \quad t > 0 \tag{17}$$

3. METHOD OF SOLUTION

To solve equations (12-14), we assume solution of the form

$$u(y,t) = \left[u_0(y) + \varepsilon \exp(i\omega t) u_1(y)\right] \tag{18}$$

$$\theta(y,t) = \left[\theta_0(y) + \varepsilon \exp(i\omega t)\theta_1(y)\right] \tag{19}$$

$$C(y,t) = \left[C_0(y) + \varepsilon \exp(i\omega t) C_1(y)\right] \tag{20}$$

where ε is a small parameter

Case 1: Both walls of the channel are kept stationary, while the temperature of the upper wall of the channel is assumed constant, the lower wall has uniform temperature and the boundary conditions conform to equations 18-20. We substitute equation (20) into equation (14) and simplify, the result is

$$C_0''(y) - c_2 C_0(y) = 0 \tag{21}$$

$$C_1''(y) - (c_1 i\omega + c_2) C_1(y) = 0 \tag{22}$$

Solving equations (21) and (22) and imposing the boundary conditions of equation (17) as well as substituting in equation (20), we get

$$C(y,t) = Sinh\sqrt{c_2}\, y + \varepsilon \exp(i\omega t) Sinh\sqrt{\beta}\, y \tag{23}$$

where $\beta = c_1 i\omega + c_2$

Similarly, we put equation (19) into equation (13) and the resulting expression takes the form

$$\theta_0''(y) - b_2\theta_0(y)0 = 0 \tag{24}$$

$$\theta_1''(y) - (b_1 i\omega + b_2)\theta_1(y) = 0 \tag{25}$$

The solutions of equations (24) and (25) and imposition of the boundary conditions of equation (16) as well as put the entire expression into equation (19), gives

$$\theta(y,t) = Sinh\sqrt{b_2}\, y + \varepsilon \exp(i\omega t) Sinh\sqrt{\beta_2}\, y \tag{26}$$

where $\beta_2 = b_1 i\omega + b_2$

Also, following the same procedure and the boundary conditions of equation (18), the solution of equation (12) is

$$u(y,t) = \beta_5 Sinh\sqrt{\frac{a_2}{w_2}}\, y + \beta_3 Sinh\sqrt{b_2}\, y + \beta_4 Sinh\sqrt{c_2}\, y + \varepsilon \exp(i\omega t)\left(-\beta_8 Cosh\sqrt{\frac{a_1+a_2}{w_2}}\, y + \beta_9 Sinh\sqrt{\frac{a_1+a_2}{w_2}}\, y + \beta_6 Sinh\sqrt{\beta_2}\, y + \beta_7 Sinh\sqrt{\beta}\, y + \beta_8\right) \tag{27}$$

where, $\beta_3 = \dfrac{-\frac{a_3}{w_2}}{b_2^2 - \frac{a_2}{w_2}}$, $\beta_4 = \dfrac{a_4}{w_2(c_2^2 - 1)}$, $\beta_5 = \dfrac{-\beta_3 Sinh\sqrt{b_2} - \beta_4 Sinh\sqrt{c_2}}{Sinh\sqrt{\frac{a_2}{w_2}}}$, $\beta_6 = \dfrac{-\frac{a_3}{w_2}}{\beta_2 - \frac{a_1+a_2}{w_2}}$,

$\beta_7 = \dfrac{-\frac{a_4}{w_2}}{\beta - \frac{a_1+a_2}{w_2}}$, $\beta_8 = \dfrac{\lambda}{a_1+a_2}$, $\beta_9 = \dfrac{-\left(\beta_8 + \beta_6 Sinh\sqrt{\beta_2} + \beta_7 Sinh\sqrt{\beta}\right)}{Sinh\sqrt{\frac{a_1+a_2}{w}}}$

Case 2: The upper wall of the channel is set into oscillatory motion while the lower wall is held stationary and the resulting boundary conditions are given as

$$u(0,t)=0, \text{ and } u(1,t)=H(t)\varepsilon\exp(i\omega t); \quad t>0 \tag{28}$$

where H(t) is the Heaviside step function.

Imposing the boundary conditions of equation (28) into the solution of equation (12), we get

$$\begin{aligned} u(y,t) &= \left(\frac{H(t)\varepsilon\exp(i\omega t)-\beta_3 Sinh\sqrt{b_2}-\beta_4 Sinh\sqrt{c_2}}{Sinh\sqrt{\frac{a_2}{w_2}}}\right)Sinh\sqrt{\frac{a_2}{w_2}}y \\ &+\beta_3 Sinh\sqrt{b_2}\,y+\beta_4 Sinh\sqrt{c_2}\,y \\ &+\varepsilon\exp(i\omega t)\left[\left(\frac{H(t)\varepsilon\exp(i\omega t)-\beta_6 Sinh\sqrt{\beta_2}-\beta_7 Sinh\sqrt{\beta}-\beta_8}{Sinh\sqrt{\frac{a_1+a_2}{w_2}}}\right)Sinh\sqrt{\frac{a_1+a_2}{w_2}}y+\beta_{10}\right] \end{aligned} \tag{29}$$

where $\beta_{10}=\beta_6 Sinh\sqrt{\beta_2}\,y+\beta_7 Sinh\sqrt{\beta}\,y+\beta_8$

Case 3: In this situation, the two channel walls are set into oscillatory motion and the resulting boundary conditions Aiza et al. [18] are given as

$$u(0,t)=H(t)\varepsilon\exp(i\omega t) \text{ and } u(1,t)=H(t)\varepsilon\exp(i\omega t) \;\; t>0 \tag{30}$$

The solution of equation (12), having used the boundary conditions of equation (30), following the same procedure used in case 2, we obtain

$$\begin{aligned} u(y,t) &= H(t)\varepsilon\exp(i\omega t)Cosh\sqrt{\frac{a_2}{w_2}}y+ \\ &\left(\frac{H(t)\varepsilon\exp(i\omega t)-\beta_3 Sinh\sqrt{b_2}-\beta_4 Sinh\sqrt{c_2}}{Sinh\sqrt{\frac{a_2}{w_2}}}\right)Sinh\sqrt{\frac{a_2}{w_2}}y \\ &+\beta_3 Sinh\sqrt{b_2}\,y+\beta_4 Sinh\sqrt{c_2}\,y \\ &+H(t)\varepsilon\exp(i\omega t)Cosh\sqrt{\frac{a_1+a_2}{w_2}}y+ \\ &\left(\frac{H(t)\varepsilon\exp(i\omega t)-\beta_6 Sinh\sqrt{\beta_2}-\beta_7 Sinh\sqrt{\beta}-\beta_8}{Sinh\sqrt{\frac{a_1+a_2}{w_2}}}\right)Sinh\sqrt{\frac{a_1+a_2}{w_2}}y \\ &+\beta_6 Sinh\sqrt{\beta_2}\,y+\beta_7 Sinh\sqrt{\beta}\,y+\beta_8 \end{aligned} \tag{31}$$

Nusselt number (Nu) (the rate of heat transfer coefficient)

From equation (26), the Nusselt number is given by

$$Nu = -\left(\frac{\partial\theta}{\partial y}\right)_{y=0} = -\left(\sqrt{b_2} + \varepsilon\exp(i\omega t)\sqrt{\beta_2}\right) \tag{32}$$

Sherwood number (S_b)(the rate of mass transfer coefficient)

$$S_b = -\left(\frac{\partial C}{\partial y}\right)_{y=0} = -\left(\sqrt{C_2} + \varepsilon\exp(i\omega t)\sqrt{\beta}\right) \tag{33}$$

Skin frictions (τ)

$$\left(\frac{\partial u}{\partial y}\right)_{y=0} = \beta_5\sqrt{\frac{a_2}{w_2}} + \beta_3\sqrt{b_2} + \beta_4\sqrt{c_2} + \varepsilon\exp(i\omega t)\left(\beta_9\sqrt{\frac{a_1+a_2}{w_2}} + \beta_6\sqrt{\beta_2} + \beta_7\sqrt{\beta}\right) \tag{34}$$

Case 2

$$\left(\frac{\partial u}{\partial y}\right)_{y=0} = \left(\frac{H(t)\varepsilon\exp(i\omega t) - \beta_3 Sinh\sqrt{b_2} - \beta_4 Sinh\sqrt{c_2}}{Sinh\sqrt{\frac{a_2}{w_2}}}\right)\sqrt{\frac{a_2}{w_2}} + \beta_3\sqrt{b_2} + \beta_4\sqrt{c_2} + \varepsilon\exp(i\omega t)\left[\left(\frac{H(t)\varepsilon\exp(i\omega t) - \beta_6 Sinh\sqrt{\beta_2} - \beta_7 Sinh\sqrt{\beta} - \beta_8}{Sinh\sqrt{\frac{a_1+a_2}{w_2}}}\right)\sqrt{\frac{a_1+a_2}{w_2}} + \beta_{77}\right] \tag{35}$$

where $\beta_{77} = \beta_6\sqrt{\beta_2} + \beta_7 Sinh\sqrt{\beta}$

Case 3

$$\left(\frac{\partial u}{\partial y}\right)_{y=0} = \left(\frac{H(t)\varepsilon\exp(i\omega t) - \beta_3 Sinh\sqrt{b_2} - \beta_4 Sinh\sqrt{c_2}}{Sinh\sqrt{\frac{a_2}{w_2}}}\right)\sqrt{\frac{a_2}{w_2}} + \beta_3\sqrt{b_2} + \beta_4\sqrt{c_2} + \left(\frac{H(t)\varepsilon\exp(i\omega t) - \beta_6 Sinh\sqrt{\beta_2} - \beta_7 Sinh\sqrt{\beta} - \beta_8}{Sinh\sqrt{\frac{a_1+a_2}{w_2}}}\right)\sqrt{\frac{a_1+a_2}{w_2}} + \beta_6\sqrt{\beta_2} + \beta_7\sqrt{\beta} \tag{36}$$

4. DISCUSSION

As a result of increase in the chemical reaction of the nanoparticles and the base fluid, a corresponding increase in the concentration of the nanofluid is observed as depicted in Fig. 1.

Fig. 2 shows, the effect of radiation on the temperature of copper nanofluid. As a result of high thermal conductivity of nanofluid, increase in radiation of nanofluid result in a corresponding increase in the temperature profile of the nanofluid. This observation is consistent with the work of Aaiza et al. [18] and Timofeeva et al. [30] and a departure from the effect of radiation on other base fluids.

Fig. 3 shows, the convective heat transfer coefficient between the nanofluid and the channel walls to estimate the heat transfer performance of the nanofluid. The graph showed that, the heat transfer is rapid (a curve), may be due to the presence of radiation when compared to the work of Xuan and Li [31] which is a straight line. The peclet number is a parameter to describe such effect. Equation (32) therefore, is a holistic approach to study the improved heat transfer mechanism of the nanofluid.

From Fig. 4 it is shown, that the relationship can be used to determine the convective mass transfer coefficient between the nanofluid and the containing inner wall to estimate the improved mass transfer performance of the nanoparticles.

Fig. 5 demonstrates clearly that the increase in peclet number corresponds to a decrease in the skin friction of the nanofluid.

Increase in nanoparticles volume fraction of copper nanofluid result in a corresponding increase in the velocity profile of the nanofluid as shown in Fig. 6.

Reynolds number describe the transition of fluids from laminar to turbulence, since it is a ratio of inertia force to viscous force, its increase as shown in Fig. 7, results in a decrease in the velocity profile of nanofluid and this observation is at variance with the results of increase in Reynolds number of base fluids Ngiangia and Harry [26].

Electroconductivity tends to impede the flow of fluid and same observation was noticed as depicted in Fig. 8, where increase in electroconductivity enhances the decrease in the velocity of copper nanofluid.

The Grashof number due to temperature conducts heat away from the channel plates into the nanofluid, thereby increasing the temperature of the fluid but as a result of rapid heat transfer and thermal conductivity of nanofluid, a decrease in velocity profile of the nanofluid is observed as shown in Fig. 9.

Fig. 10 shows, the effect of different shapes of copper nanoparticles on the velocity of water based nanofluids. The graph clearly depicts that, the highest velocity is recorded with brick followed by cylinder, platelet and finally blade. The effect on shapes of nanoparticles on velocity is also a dependence on viscosity for various volume fractions.

The following numerical values are used in the plotting of the graphs

$$\lambda_n = 100, \omega = 0.2, t = 1, \lambda = 1, \varepsilon = 0.003, k = 0.3$$
$$Gr_T, Gr_C = 1,3,5,7$$
$$Pe = 0.35,0.70,1.05,1.40$$
$$\phi = 0.1,0.2,0.3,0.4$$
$$\mathrm{Re} = 100,1500,2000,2500$$
$$N = 2.0,4.0,6.0,8.0$$
$$k_\infty = 1.35,2.35,3.35,4.45$$
$$\sigma_0 = 0.4,0.8,1.2,1.6$$

Table 1. Constants a and b empirical shape factors, Timofeeva et al. [30]

Model	Platelet	Blade	Cylinder	Brick
a	37.1	14.6	13.5	1.9
b	612.6	123.3	904.4	471.4

Table 2. Sphericity for different shapes nanoparticles, Timofeeva et al. [30]

Model	Platelet	Blade	Cylinder	Brick
ψ	0.52	0.36	0.62	0.81

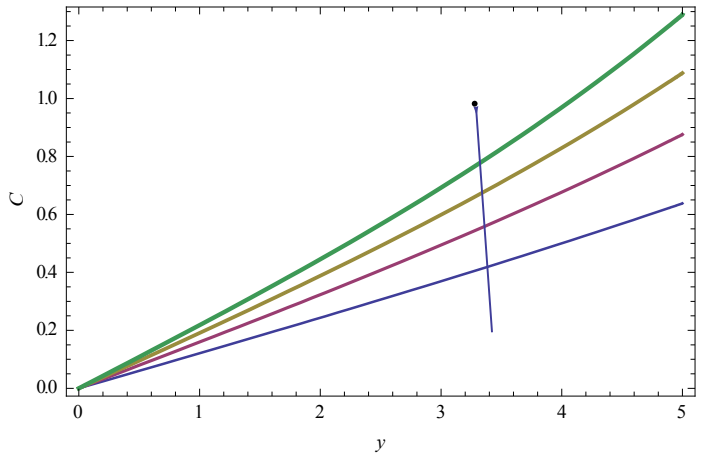

Fig. 1. The dependence of concentration on coordinate with chemical reaction k_∞ varying

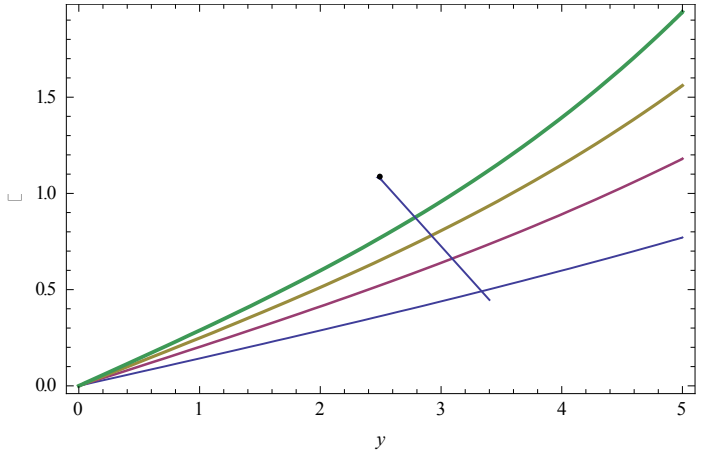

Fig. 2. The dependence of temperature on coordinate with radiation N varying

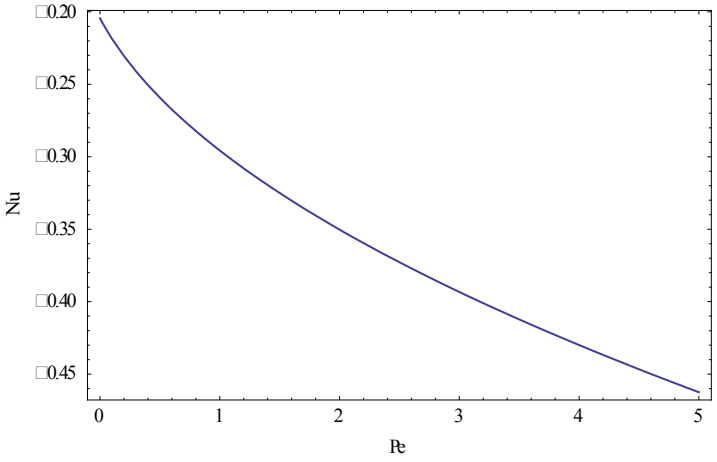

Fig. 3. The Nusselt number (Nu) versus Peclet number(Pe)

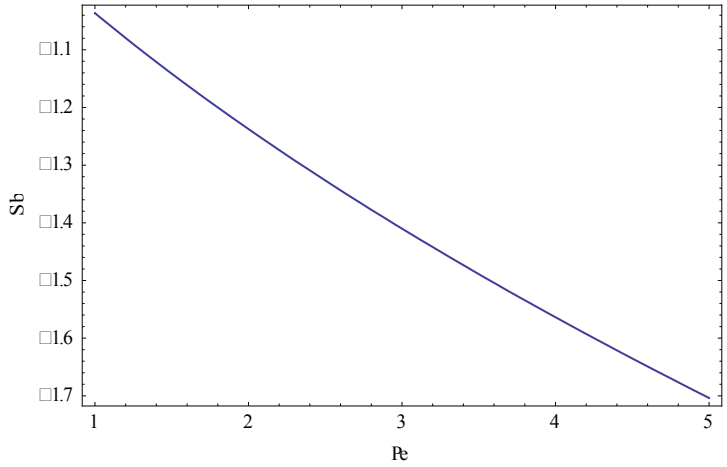

Fig. 4. The Sherwood number (Sb) versus Peclet number(Pe)

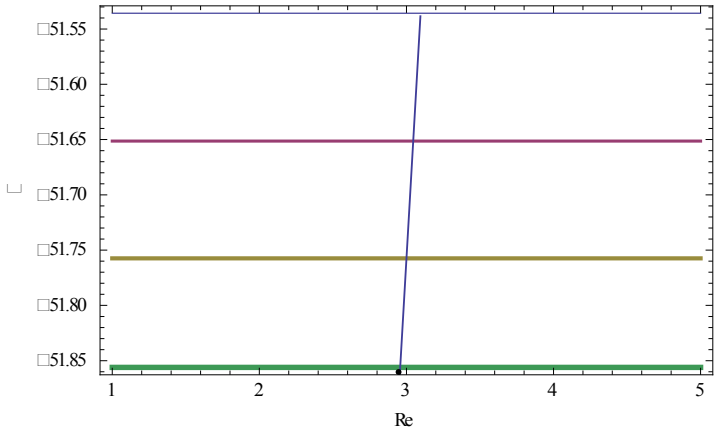

Fig. 5. The Skin Friction (τ) versus Reynolds number (Re) with Peclet number(Pe) varying.

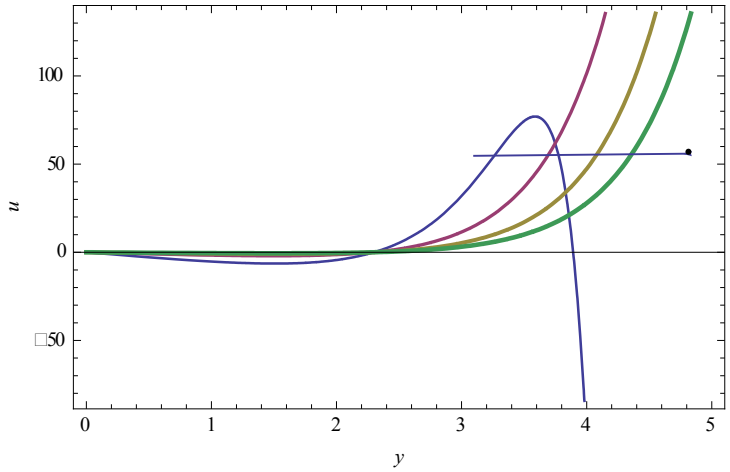

Fig. 6. The dependence of velocity on coordinate with nanoparticles volume fractions ϕ varying

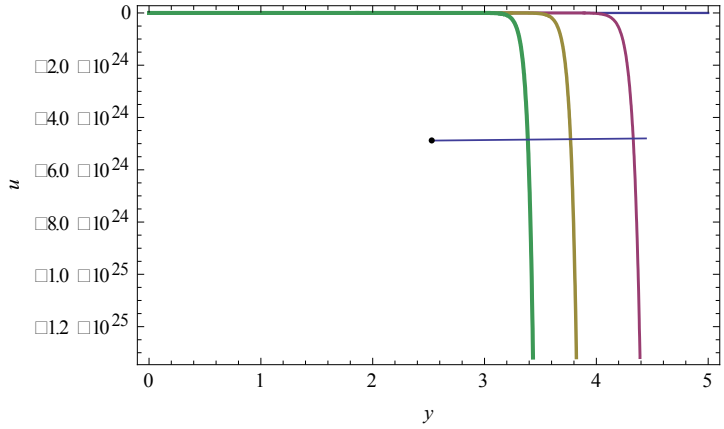

Fig. 7. The dependence of velocity on coordinate with Reynolds number Re varying

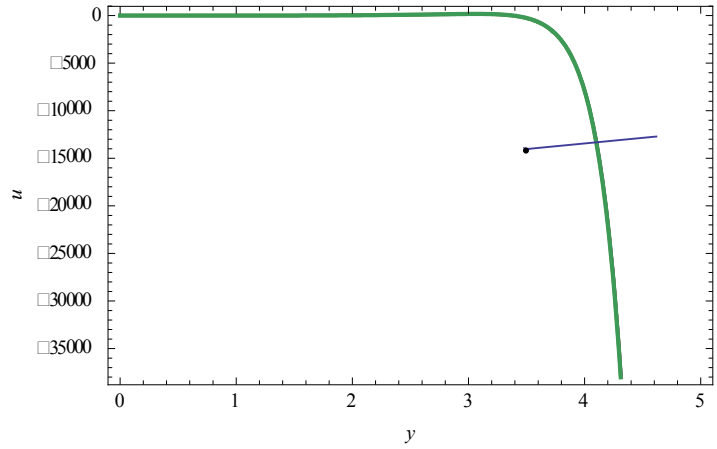

Fig. 8. The dependence of velocity on coordinate with conductivity σ_0 varying

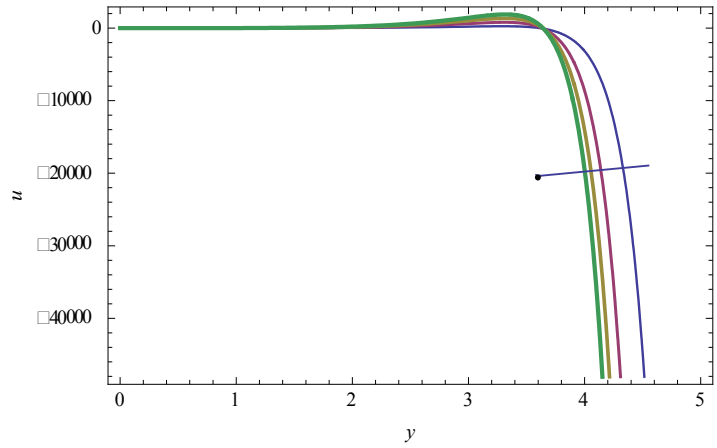

Fig. 9. The dependence of velocity on coordinate with Grash of number Gr_T varying

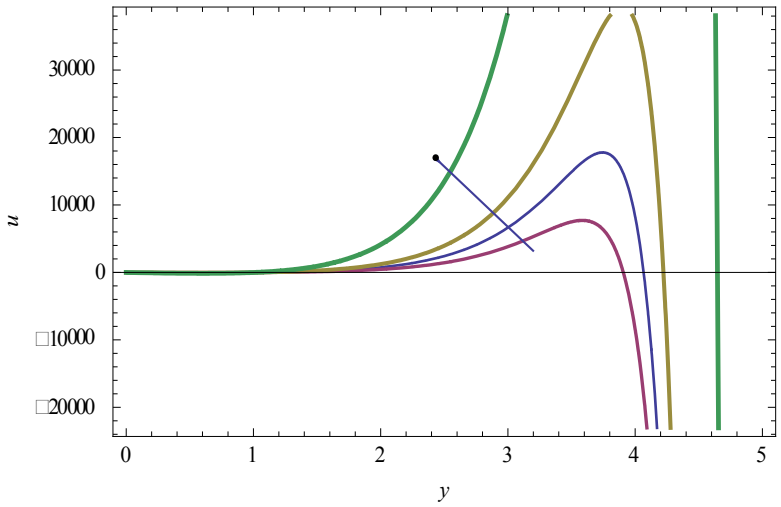

Fig. 10. The dependence of velocity on coordinate with different nanoshape particles n

Table 3. Thermophysical properties of water and nanoparticle, Timofeeva et al. [30]

Model	$\rho(kgm^{-3})$	$C_p(kg^{-1}K^{-1})$	$k(Wm^{-1}K^{-1})$	$\beta x10^{-5}K^{-1}$
Water (H_2O)	997.1	4179	0.613	21
Copper (Cu)	8933	385	401	1.67

5. CONCLUSIONS

A perturbation technique on the description of the heat and mass transfer of copper nanofluid has been carried out. An essential characteristic of nanofluid, in particular copper nanoparticles in water based fluids is that, as a result of its high thermal conductivity and heat transfer ability, the effect on velocity profile is significantly different from other conventional base fluids. Though the results are in substantial agreement with other published works, experiments is needed for industrial, scientific and engineering applications of copper nanaofluid and others. It should be noted that the improved performance of the copper nanofluid is not limited to its high thermal conductivity and heat transfer ability but also from the random movement and dispersion effect on the nanoparticles. The effect of Grashof number on the concentration of nanofluid was ignored because the result is the same as that of the temperature.

ACKNOWLEDGEMENTS

Authors extended their heartfelt appreciation to the reviewers for their valuable suggestion for the improvement of the article

COMPETING INTERESTS

Authors have declared that no competing interests exist.

REFERENCES

1. Touloukian YS, Powell RW, Ho CY, Klemens PG. Thermophysical properties of matter. Plenum Press, New York. 1970;2.
2. Choi US. Enhancing thermal conductivity of fluids with nanoparticles. Development and Applications of Non-Newtonian Flows. Eds. D. A. 1995;99-105.
3. Choi US, Cho YI, Kasza KE. Degradation effects of dilute polymer solutions on turbulent friction and heat transfer behavior. Journal of Non-Newtonian Fluid Mechanics. 1992a;41:289 -307.
4. Choi US, France DM, Knodel BD. Impact of advanced fluids on costs of districts cooling systems. Proceedings of 83rd Annual International Districts Heating and Cooing Association Confrence. Danves, Washington D C. 1992b;343-359.
5. Mukherjee S, Paria S. Preparation and Stability of Nanofluids-A Review. IOSR

Journal of Mechanical and Civil Engineering. 2013;9(2):63-69.

6. Feng X, Ma H, Huang S. Aqueous-organic phase-transfer of highly stable gold, silver, and platinum nanoparticles and new route for fabrication of gold nanofilms at the oil/water interface and on solid supports. Journal of Physical Chemistry B. 2006; 110(25):12311–12317.
7. Yu W, Xie H, Chen L, Li L. Enhancement of thermal conductivity of kerosene-based Fe_3O_4 nanofluids prepared via phase-transfer method. Colloids and Surfaces A. 2010;355(1–3):109–113.
8. Wei X, Wang L. Synthesis and thermal conductivity of microfluidic copper nanofluids, Particuology. 2010;8(3):262–271.
9. Zhu HT, Zhang CY, Tang YM, Wang JX. Novel synthesis and thermal conductivity of CuO nanofluid. Journal of Physical Chemistry C. 2007;111(4):1646–1650.
10. Hwang Y, Lee JK, Lee CH. Stability and thermal conductivity characteristics of nanofluids, Thermochimica Acta. 2007; 455(1-2):70–74.
11. Li X, Zhu D, Wang X. Evaluation on dispersion behavior of the aqueous copper nanosuspensions,‖ Journal of Colloid and Interface Science. 2007;310(2):456–463.
12. Hussain S, Muhammad S, Ali G, Naeem M. A bioconvection model for squeezing flow between parallel plates containing gyrotactic microorganisms with impact of thermal radiation and heat generation/ absorption. Journal of Advances in Mathematics and Computer Science. 2018;27(4):1-22.
13. Muhammad S, Shah SIA, Ali G, Ishaq M, Hussain SA, Shah Z. Effect of thermal radiation on burgers nano fluid flow between two parallel plates with porous medium in the presence of gyrotactic micro-organisms and heat generation /absorption. Journal of Nanofluids. 2018a; 8(5):957-969.
14. Muhammad S, Shah SIA, Ali G, Ishaq M, Hussain SA, Ullah H. Squeezing nanofluid flow between two parallel plates under the influence of MHD and thermal radiation. Asian Research Journal of Mathematics. 2018b;10(1):1-20.
15. Muhammad S, Ali G, Shah Z, Islam S, Hussain S. The rotating flow of magneto hydrodynamic carbon nanotubes over a stretching sheet with the impact of non-linear thermal radiation and heat generation/absorption. Journal of Applied Sciences. 2018c;8(4):482-493.
16. Hamilton RL, Crosser OK. Thermal conductivity of heterogeneous two-component systems. Journal of Industrial and Engineering Chemistry Fundamentals. 1962;1(3):187-191.
17. Li BC. Nanotechnology in China. Journal of Aerosol Science. 1998;29(5/6): 751-755.
18. Aaiza G, Khan I, Shafie S. Energy transfer in mixed convection MHD flow of nanofluid containing different shapes of nanoparticles in a channel filled with saturated porous medium. Nanoscale Research Letters. 2015;10(490):1-4.
19. Asma K, Khan I, Sharidan S. Exact solutions for free convection flow of nanofuids with ramped wall temperature. The European Physical Journal Plus. 2015;130:57-71.
20. Sebdani S, Mahmoodi M, Hashemi S. Effect of nanofluid variable properties on mixed convection in a square cavity. International Journal of Thermodynamic Science. 2012;52:112-126.
21. Sheikhzabeh GA, Hajialigol N, Qomi ME, Fattahi A. Laminar mixed convection of cu-water nanofluid in two sided lid-driven enclosures. Journal of Nanostuctures. 2012;1:44-53.
22. Nadeem S, Saleem S. Unsteady mixed convection flow of nanofluid on a rotating cone with magnetic field. Apply Nanoscience. 2004;4:405-414.
23. Al-Salem K, Oztop HF, Pop I, Varo Y. Effect of moving lid direction on MHD mixed convection in a linearly heated cavity. International Journal of Heat and Mass Transfer. 2012;55:1103-1112.
24. Yimin Xuan, Li Q. Heat transfer enhancement of nanofluids‖. International Journal of Heat and Fluid Flow. 2000;21:58-64.
25. Boricic Z, Nikodijevic D, Milenkovic D, Stamenkovic Z. A form of MHD universal equation of unsteady incompressible fluid flow with variable electroconductivity on heated moving plate. Theoretical and Applied Mechanics. 2005;32(1):65-77.
26. Ngiangia AT, Harry ST. Electroconductivity of Steady viscous MHD incompressible fluid between two porous parallel plates provoked by chemical reaction and radiation. Physical Science International Journal. 2017;13(2):1-13.

27. Wasp F. Solid-liquid flow slurry pipeline transportation. Trans. Tech. Pub. Berlin; 1977.
28. Makinde OD, Mhone PY. Heat transfer to MHD oscillatory flow in a channel filled with porous medium. Romanian Journal of Physics. 2005;50:931-938.
29. Cogley AC, Vincent WG, Giles SE. Differential approximation to radiative heat transfer in a non-grey gas near equilibrium. The American Inst. Aeronautics and Astronautics. 1968;6:551–553.
30. Timofeeva EV, Routbort JL, Singh D. Particle shape effects on thermophysical properties of alumina nanofluids. Journal of Applied Physics. 2009;106(1): 014304.
31. Xuan Y, Li Q. Heat transfer enhancement of nanofuids. International Journal of Heat and Fluid Flow. 2000;21:58-64.

Peer-review history:
The peer review history for this paper can be accessed here:
http://www.sdiarticle3.com/review-history/46301